

Starbursts and AGN in Luminous Infrared Galaxies

L. Armus

Spitzer Science Center, Caltech

Abstract. Luminous Infrared Galaxies (LIRGs), which emit a significant fraction of their bolometric luminosity in the far-infrared, have $L_{IR} \geq 10^{11}L_{\odot}$. LIRGs are a mixture of single galaxies, disk galaxy pairs, interacting systems, and advanced mergers which exhibit enhanced star-formation rates and AGN activity compared to normal galaxies. At the highest luminosities ($L_{IR} \geq 10^{12}L_{\odot}$), Ultraluminous Infrared Galaxies (ULIRGs) may represent an important stage in the formation of QSOs. If the growth of the central black hole preferentially occurs during periods of enhanced star formation, LIRGs and ULIRGs are important laboratories in which to understand both processes. The Great Observatories All-Sky LIRG Survey (GOALS) is aimed at measuring the properties of a large, complete sample of low-redshift LIRGs across the electromagnetic spectrum. With its ability to probe the stars, dust and ionized and molecular gas in LIRGs through mid-infrared imaging and spectroscopy, Spitzer is providing a key component of the GOALS data. In this paper, we summarize the key findings from Spitzer Infrared Spectrograph (IRS) studies of ULIRGs at low and high redshifts, and present early results from GOALS in the context of the co-evolution of starbursts and AGN.

1. Introduction

Galaxies experiencing powerful bursts of star formation are usually blanketed in a great deal of dust. The dust reprocesses X-ray and UV photons, producing mid and far-infrared emission. The most luminous star-forming galaxies have typically been discovered via their enhanced infrared emission (Soifer et al. 1984, 1986). These galaxies can emit more than 90% of their total energy in the far-infrared part of the spectrum.

Studies with ISO and Spitzer have shown that Luminous Infrared Galaxies (LIRGs – galaxies having infrared luminosities $L_{IR} \geq 10^{11}L_{\odot}$ account for about 50% of the co-moving infrared luminosity density at $z \sim 1$ (Caputi et al. 2007; Magnelli et al. 2009), with Ultraluminous Infrared Galaxies (ULIRGs – galaxies with infrared luminosities $L_{IR} \geq 10^{12}L_{\odot}$ making up an increasing fraction at higher redshifts. More than half of all the light emitted from stars is absorbed by dust and re-radiated in the infrared (Elbaz & Cesarsky 2003).

Models and observations of luminous starbursts and AGN suggest that periods of significant mass accretion onto a central black hole may also preferentially occur during episodes of enhanced nuclear star-formation (Soltan 1982; Yu & Tremaine 2002; Hopkins et al. 2007). This seems to be borne out through studies of ULIRGs and QSOs at high redshift. Stacking of faint $1 < z < 3$ ULIRGs selected with Spitzer at $24\mu\text{m}$ suggest a significant contribution from buried AGN to the total power emitted in the far-infrared (Papovich, et al. 2007; Daddi, et al. 2007). The recent discovery of resolved far-infrared [C II]

emission in the $z = 6.42$ QSO SDSS J114816.6+52, suggests a star-formation rate of about $1700M_{\odot} \text{ yr}^{-1}$ (Walter et al. 2009), providing further evidence for the link between black hole and stellar bulge growth at extremely high-redshift.

LIRGs and ULIRGs in the local Universe provide a critical laboratory for understanding the processes that drive powerful starbursts and fuel growing black holes at high redshift. Nearly all low-redshift ULIRGs are interacting or merging, late-type galaxies. ULIRGs have intense, compact nuclear starbursts and many appear to harbor (buried) AGN. Some ULIRGs have such intense nuclear star-formation that they also drive winds of hot gas into the galactic halo. In the simplest model of ULIRG evolution, a merger triggers an intense starburst and the fueling of a nascent AGN. The earliest stages are starburst-dominated with cool far-infrared colors. As the molecular fuel is used up and the AGN begins to dominate the emission, the far-infrared colors become warmer, eventually revealing the central QSO as the dust is cleared through the action of SNe and the AGN itself (see Sanders & Mirabel 1996 for a review).

An important question has always been the nature of the dominant energy source powering the dust emission in ULIRGs. How many ULIRGs are AGN dominated, how many are starburst dominated, and how many are composite systems (with a significant contribution from young stars and a central AGN)? Are the relative fractions consistent with the simple model of their evolution? Do these fractions evolve with redshift, and are the basic properties of low-redshift ULIRGs and LIRGs similar to those at high-redshifts?

2. Low-Redshift ULIRG Spectroscopy with Spitzer

The sensitivity and broad mid-infrared wavelength coverage of the Infrared Spectrograph (IRS - see Houck et al. 2004) has provided us with the opportunity to study large numbers of low-redshift LIRGs and ULIRGs. There are a number of advantages of the mid-infrared for addressing some of the fundamental questions regarding ULIRGs. Compared to the visual, the extinction in the mid-infrared is greatly reduced, and there are numerous atomic, fine-structure lines (e.g., [Ne II], [Ne III], [Ne V], [O IV], [S III]) that are effective diagnostics of the radiation field. In particular, since the ionization potential of Ne^{++++} is 97 eV, this usually signals the presence of an AGN in the spectrum of a galaxy. In addition, pure rotational lines of H_2 are available as direct probes of the warm (100-400 K) molecular gas. Finally, aromatic features (Poly-cyclic Aromatic Hydrocarbons) are abundant, the strongest being at 6.2, .7, 8.6, 11.3, 12.7, and $17\mu\text{m}$. These small grains are easily destroyed in the harsh radiation fields surrounding an AGN, yet are ubiquitous in star-forming galaxies. The fine-structure line ratios together with the PAH features provide a powerful diagnostic of the dominant energy source in a dusty galaxy, first demonstrated effectively with data from the Infrared Space Observatory (Genzel, et al. 1998; Sturm et al. 2002).

Well over 100 low-redshift ULIRGs have been observed with the IRS on Spitzer (Armus et al. 2004, 2006, 2007; Higdon, et al. 2006; Desai et al. 2007, Spoon et al. 2004, 2007; Imanishi et al. 2007; Farrah et al. 2007). The most striking aspect of the low-resolution (Short-Low and Long-Low) spectra are their diversity. The mid-infrared spectra of ULIRGs range from nearly featureless, power-law spectra (with and without silicate absorption) to those that are dominated by very strong PAH and fine-structure line emission. In

the low-resolution spectra, PAH emission, and H₂O, hydrocarbon, and silicate absorption are the dominant spectra features. In many of the low-resolution spectra, the fine-structure lines of [Ne II] 12.8 μ m, [Ne III] 15.5 μ m, [O IV] 25.9 μ m, [S II] 18.7, 33.4 μ m, and [Si II] 34.8 μ m can also be seen. The power-law spectra are most easily explained as produced in ULIRGs where an AGN dominates the mid-infrared emission. The PAH-rich spectra are produced in ULIRGs where star-formation dominates. From the silicate absorption at 9.7 and 18 μ m, the implied visual extinctions range from undetectable, to $A_V > 80$ mag. The strength of the silicate absorption also appears correlated with the 6.2 μ m PAH equivalent width (EQW), such that ULIRGs with low PAH EQW can have either very small or very large silicate absorption (Spoon et al. 2007). The lack of a significant number of ULIRGs with intermediate silicate absorption depth at low PAH EQW might indicate a short timescale for this stage once the hot dust becomes visible.

The mid-infrared spectra of ULIRGs roughly correlate with the optical classification. Sources that are classified based upon their optical emission line ratios as either Seyferts or QSOs have smaller PAH EQW (on average), than do sources which are classified as starbursts (Desai et al. 2007). The Seyfert ULIRGs have a median 6.2 μ m PAH EQW of 0.04 μ m, while the starburst ULIRGs have a median 6.2 μ m PAH EQW of 0.28 μ m. ULIRGs that are optically classified as LINERs fall in between, having a median 6.2 μ m PAH EQW of 0.11 μ m. Similarly, ULIRGs which are classified as “cold” in the far-infrared (ratio of IRAS $f_{25}/f_{60} < 0.2$) have a median 6.2 μ m PAH EQW (0.24 μ m) which is significantly larger than that seen in “warm” ULIRGs (0.04 μ m). While there is rough consistency between optical and mid-infrared spectral types, there are important differences among individual sources, the classes as a whole. For example, the median 6.2 μ m PAH EQW among the ULIRGs that are optically classified as starbursts, is only about half as large as that seen in pure starburst galaxies of lower luminosity (Brandl et al. 2006).

There are also trends of the PAH EQW with luminosity among ULIRGs. The lowest luminosity sources tend to have the largest PAH EQW, closest to that seen in pure starburst galaxies, while the most luminous sources have the smallest PAH EQW (Desai et al. 2007). This trend had also been seen in the ISO data (Tran et al. 2001). The low PAH EQW in the most luminous ULIRGs is consistent with an excess of hot dust in these galaxies. The relation, although it has a large scatter, can be fit by $\log_{10}[6.2\mu\text{m PAH EQW } (\mu\text{m})] = (7.71 \pm 0.07) + (-0.723 \pm 0.006) \times \log_{10}(\nu L_{24}) [L_{\odot}]$.

The IRS high-resolution data show that about 40% of the ULIRGs show [NeV] emission. The faintest lines confidently observed have fluxes around $10^{-21} \text{ W cm}^{-2}$, and line flux ratios of [NeV] 14.3/[NeII] 12.8 = 0.01 (Armus et al. 2004, 2007; Farrah et al. 2007). The AGN fraction implied from strengths of either the [NeV] or [OIV] emission lines is often significantly lower than implied by the 6.2 μ m PAH EQW, or L_{PAH} / L_{IR} . About 10% of the sources with detectable [NeV] emission are classified as starbursts in the optical, while the rest are either LINERs or Seyferts. Interestingly, [NeV] emission is detected even in some sources that are optically thick as measured in the X-rays (e.g. NGC 6240, UGC 5101), and it is not seen in some sources that are type-1 AGN in the optical (e.g. Mrk 231).

Although the $6.2\mu\text{m}$ PAH EQW is an extremely effective diagnostic of the importance of an AGN to the mid-infrared spectrum, the total to mid-IR emission and the PAH band ratios vary from ULIRG to ULIRG. By measuring all the PAH features and the total IR emission from the ULIRGs, we can estimate the fraction of the total energy generated by young stars. When the full ULIRG spectral energy distributions are fit according to the method outlined in Marshall et al. (2007), the ratio of total PAH to IR luminosity can be measured for each source. The result is shown in Figure 1. The L_{PAH}/L_{IR} ratio in ULIRGs ranges from about 0.004 to 0.09 in the sample. Arp 220 has the lowest value, while IRAS 18030+0705 has the largest. Since the bolometric energy in ULIRGs is dominated by the infrared, this is equivalent to the fraction of the total power produced by young stars. If we look at the ULIRGs as a class, and compare them to pure starburst galaxies, the median value of L_{PAH}/L_{IR} suggests that approximately 40-50% of the energy of a typical ULIRG is generated from a starburst. Studies of PG QSOs (Schweitzer et al. 2006, 2008) also suggest that up to 30% of the far-infrared luminosity could be generated by a starburst, but in these systems, this only accounts for a few percent of the bolometric luminosity.

Although it has been known for quite some time that ULIRGs can drive powerful outflows (e.g., Heckman, Armus & Miley 1990; Heckman et al. 2000), the IRS high-resolution data has recently been used to penetrate the dust in IRAS F00183-7111 and give us a glimpse of the high-velocity gas and shocks at the base of a superwind (Spoon et al. 2009). These winds may help clear out the circum-nuclear dust and gas in ULIRGs, speeding up their transformation from starburst to QSO.

3. High-Redshift ULIRG Spectroscopy with Spitzer

There have been a number of programs targeting ULIRGs at high-redshift with the IRS. These sources have been selected in a wide variety of ways, from the sub-millimeter to the near-infrared. Although the numbers of galaxies observed is still relatively small (compared to the numbers observed at low-redshift) some interesting trends, and some surprises, are already evident.

The majority of bright, $24\mu\text{m}$ -selected sources (those with $f_{24} \geq 0.5$ mJy) between redshifts of $1 < z < 3$ appear to be AGN-dominated (Houck et al. 2005; Sajina et al. 2007, 2008; Yan et al. 2007). These sources typically have power-law IRS spectra, with little or no PAH emission. This AGN “bias” is naturally explained since an excess of hot dust makes AGN-like ULIRGs appear brighter in the observed mid-infrared bands at these redshifts. However, this selection effect has been overcome through a variety of means in Spitzer IRS spectral surveys by selecting (1) fainter sources ($f_{24} < 0.3$ mJy), (2) on color (based on IRAC, MIPS together with optical magnitudes, or by using IRAC colors to select sources with strong, rest-frame near-infrared stellar “bumps”), (3) sources with high infrared-to-X-ray ratios, and (4) sub-millimeter galaxies. Recent surveys of high-redshift ULIRGs with the IRS selected on these criteria (Pope et al. 2008; Valiante et al. 2007; Sajina et al. 2007; Teplitz et al. 2007; Farrah et al. 2008; Menendez-Delmestre et al. 2009; Desai et al. 2009) have uncovered samples with very strong PAH emission, indicating extremely powerful starbursts.

The IRS spectra of these high-redshift usually don’t reflect the average local ULIRG. This is understandable, given the strong selection effects and the

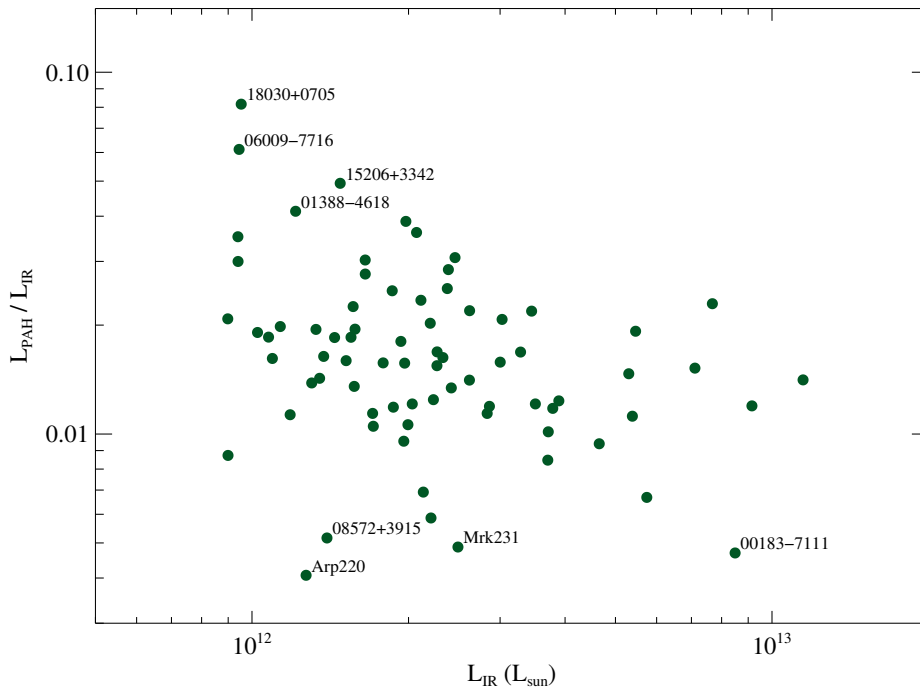


Figure 1. Total PAH to IR (8–1000 μm) luminosity ratio for local ULIRGs. The ULIRGs with the largest and smallest ratios are labeled.

limitations of the IRS. Observations of sources well below 0.5 mJy at 24 μm take many hours to complete, and the strongest PAH features as well as the silicate absorption feature are pushed out of the best part of the IRS band for $z > 3 - 3.5$. However, there do seem to be some real differences between the high and low-redshift ULIRG spectra. Very luminous starbursts (those with large PAH EQW and $L_{\text{IR}} > 10^{13} L_{\odot}$) are absent from local samples, but are seen at high redshift among the sub-millimeter and bump-selected populations. These objects fall well above the trend between 6.2 μm PAH EQW and 24 μm luminosity seen among the low-redshift ULIRGs. At low-redshift, these extremely luminous sources are almost always AGN-dominated. Perhaps not surprisingly, this is not the case at $z \sim 2$, and we see evidence for this in the IRS spectra. Also, the apparent optical depths, as measured in the silicate absorption features, for many of the luminous, starburst-dominated sub-millimeter galaxies appear lower, on average, than those seen in local ULIRGs (Pope et al. 2008; Menendez-Delmestre 2009). This may indicate more distributed star-formation in these sub-millimeter galaxies.

Studies of high-redshift galaxies with the IRS have not been restricted to ULIRGs or SMGs. In a sample of sub-millimeter detected, $z = 2$ QSOs, Lutz et al. (2008) find over 70% with PAH emission, implying star formation rates of 20 – 3000 $M_{\odot} \text{ yr}^{-1}$. Taking advantage of gravitational lensing, Rigby et al.

(2009) have presented IRS spectra of a small sample of highly magnified LIRGs at $z > 1$. A significant fraction of these LIRGs have very strong PAH emission, indicating star-formation as the dominant source of their power, although AGN may still be present at lower levels.

4. Spitzer Observations of LIRGs: The GOALS Project

While a great deal of effort has been devoted to the study of ULIRGs with the IRS, LIRGs (those galaxies with infrared luminosities above $10^{11}L_{\odot}$) have, in comparison, suffered from a lack of attention. LIRGs form a morphologically diverse group of galaxies, unlike ULIRGs which are nearly always involved in the final stages of a violent and spectacular merger. LIRGs are also much harder to detect and analyze at high redshift in many shallow surveys, which has traditionally removed much of the impetus behind establishing a robust library of low-redshift spectra. This has changed recently, with surveys such as COSMOS (Scoville et al. 2007) and GOODS (Dickinson et al. 2003), which include significant samples of LIRGs at cosmologically interesting epochs. The study of a large, complete sample of local LIRGs spanning all merger and interaction stages can shed critical light on the co-evolution of black holes and stellar bulges in massive galaxies.

The Great Observatories All-sky LIRG Survey (GOALS) combines data from NASA's Spitzer, Chandra, Hubble and GALEX observatories, together with ground-based imaging and spectroscopy, in a comprehensive survey of over 200 low redshift ($z < 0.088$) LIRGs (Armus et al. 2009). The LIRGs are a complete subset of the IRAS Revised Bright Galaxy Sample (RBGS), which comprises 629 extragalactic objects with $60\mu\text{m}$ flux densities above 5.24 Jy , and Galactic latitudes above five degrees. The LIRGs targeted in GOALS span the full range of nuclear spectral types defined via traditional optical line-ratio diagrams (type-1 and type-2 AGN, LINERs, and starbursts) as well as interaction stages (major mergers, minor mergers, and isolated galaxies). They provide an unbiased picture of the processes responsible for enhanced infrared emission in galaxies in the local Universe. The first results from GOALS are now being published, and we discuss some of the highlights here.

As expected, the mid-infrared spectra of LIRGs are intermediate between those of normal, star-forming galaxies, and ULIRGs. There is a large range in spectral shapes in the GOALS sample, from PAH dominated to continuum dominated systems. About 18% of the LIRGs show evidence for [Ne V] emission in their high-resolution IRS spectra, but only 3% have large [Ne V] $14.3 / [\text{NeII}] 12.8$ line flux ratios indicating that an AGN dominates the mid-infrared emission (Petric et al. 2009). On the other hand, about 15% of the LIRGs show very low $6.2\mu\text{m}$ PAH EQW ($< 0.3\mu\text{m}$). The IRS spectra indicate that the fraction of sources with dominant AGN is about 1/2 - 1/3 as many as seen among the local ULIRGs samples. Similarly, about 1/2 of the LIRGs with weak PAH emission (suggesting they have copious amounts of nuclear hot dust heated by and AGN) fall outside of the IRAC color locus for AGN (e.g., Stern et al. 2005) when their global IRAC colors are plotted. The AGN in these LIRGs would be missed in surveys that classify galaxies based only upon their IRAC colors.

Although LIRGs are inherently dusty, it is important to understand the range in their UV properties, because observations of LIRGs at high redshift

invariably rely on deep optical (rest-frame UV) imaging and spectroscopy to infer their properties. Through observations with HST and GALEX, GOALS is providing an important look at the far and near-UV properties of a large sample of nearby LIRGs. The median (uncorrected) far-UV luminosity among GOALS targets is $\log L_{fuv} (L_{\odot}) = 9.43$, with a range in far-UV luminosity that spans about two orders of magnitude, from $8.29 < \log L_{fuv}(L_{\odot}) < 10.31$ (Howell et al. 2009). As expected, most LIRGs have extremely large FIR to UV luminosity ratios, but there is also an extremely large spread in both the IR to UV ratio and the UV spectral slope. The log of the ratio of the far-infrared to far-UV luminosities range from 1.04 to 3.38 in GOALS, with a median value of 1.94. Estimates of the infrared luminosity of LIRGs from the UV spectral slope (β) through use of the relation for starburst galaxies (e.g., Meurer et al. 1999) will, on average, be too low by a factor of 2.4. However, use of the UV slope can also overpredict the infrared emission in a LIRG. The full range of the “error” (the true FIR divided by the predicted FIR) is between a factor of 0.2 and 33. A full discussion of the UV properties of the GOALS sample, including a presentation of the IRX- β (IR/FUV vs. UV spectral slope) relation for LIRGs is given in Howell et al. (2009).

The HST ACS and NICMOS, GALEX, and Spitzer imaging in GOALS not only provide us with global fluxes covering the UV through far-infrared, they are also allowing us to map the distribution of UV, NIR and FIR light within LIRGs. This has recently been demonstrated in a study of the merging galaxy NGC 2623 (Evans et al. 2008), where the GOALS data have been used to infer the masses and ages of ~ 100 galactic star clusters formed in the merger, as well as the buried AGN at the core of the remnant. Many merging LIRGs where the two galaxies are still resolved appear to have one galaxy which dominates the FIR (and hence the bolometric luminosity), and another galaxy that dominates the UV emission, reminiscent of the situation in VV 114 and Arp 299 (Charmandaris et al. 2004). Here we describe two examples of these types of LIRGs in GOALS, VV 340 and II Zw 096.

VV 340 (IRAS F14547+2449) consists of two large, spiral galaxies separated by approximately 27 kpc, in the early stages of a merger (Bushouse & Stanford 1992, Lo, Gao & Gruendl 1997). This system has a redshift of $z = 0.03$, and an infrared luminosity of $5 \times 10^{11} L_{\odot}$ (Sanders et al. 2003). The Spitzer MIPS imaging data indicates that about 90% of the total far-infrared emission originates in VV 340 North (Armus et al. 2009). While the IRAC colors of VV 340 North and South are consistent with star-forming galaxies, both the Spitzer IRS and Chandra ACIS data indicate the presence of an AGN in VV 340 North. Although the AGN appears to account for less than 10 – 20% of the bolometric luminosity, the X-ray data are consistent with a heavily absorbed ($N_H \geq 10^{24} \text{cm}^{-2}$) source. The GALEX far and near-UV fluxes imply a extremely large infrared “excess” (IRX) for the system ($L_{IR}/L_{fuv} \sim 81$) which is well above the correlation seen in starburst galaxies. Most of this excess is driven by VV 340 N, which has an IR excess of nearly 400. A multi-wavelength composite image of VV 340 is shown in Fig. 2.

II Zw 096 (IRAS 20550+1655) has an infrared luminosity $L_{IR} = 5.58 \times 10^{11} L_{\odot}$ and a redshift of $z=0.036$. From its morphology, II Zw 096 appears to be in the intermediate stages of a merger of at least two gas-rich spirals. Ground-based near-infrared imaging (Goldader et al. 1997) has revealed at least two,

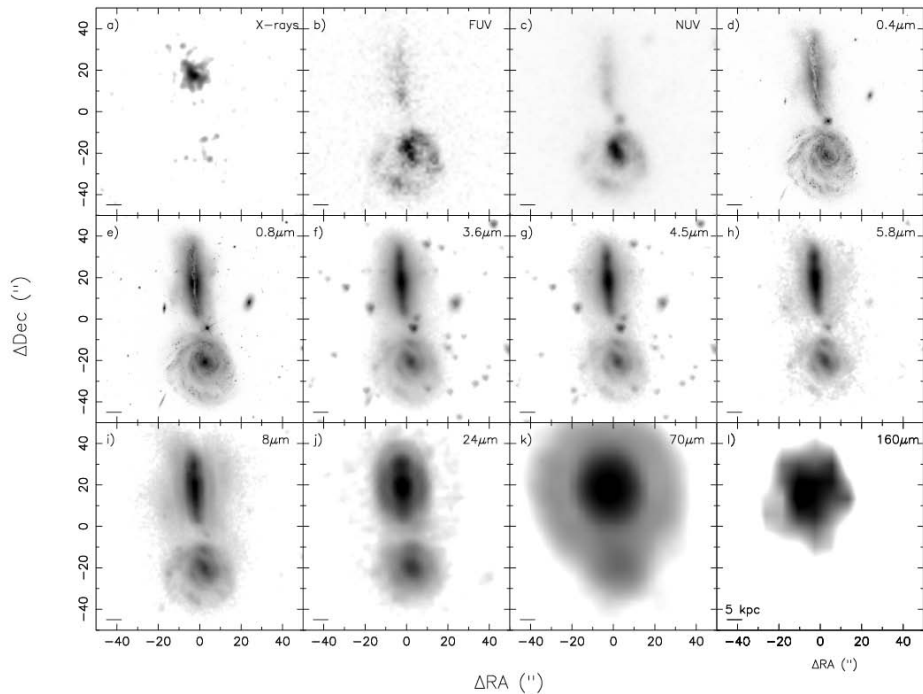


Figure 2. Multi-wavelength images of VV 340. From upper left to lower right, these are (a) Chandra 0.4–8 keV, (b) GALEX FUV, (c) GALEX NUV, (d) HST ACS F435W, (e) HST ACS F814W, (f) Spitzer IRAC 3.6 μm , (g) Spitzer IRAC 4.5 μm , (h) Spitzer IRAC 5.8 μm , (i) Spitzer IRAC 8 μm ., (j) Spitzer MIPS 24 μm , (k) Spitzer MIPS 70 μm , and (l) Spitzer MIPS 160 μm . In all cases a projected linear scale of 5 kpc at the distance of VV 340 is indicated by a bar in the lower left.

extremely red sources apparently outside of the merging nuclei. Imaging with Spitzer (Inami et al. 2009) shows that at least 80% of the total infrared luminosity comes from one of extremely red sources first identified by Goldader et al. We estimate the star formation rate (SFR) from this source to be approximately $79 M_{\odot} \text{ yr}^{-1}$. IRS spectra of this source indicates no obvious high-ionization lines from a buried AGN, although the 6.2 μm PAH equivalent width (0.20 μm) is very low for a starburst. A color image of II Zw 096 is shown in Fig. 3.

5. Conclusions

Spitzer IRS spectroscopy has revealed an unusually large diversity in the rest-frame mid-infrared spectra of ULIRGs. This is undoubtedly reflecting a wide variety of physical conditions in these extreme objects. The fact that many ULIRGs and QSOs appear composite in nature, provides evidence for periods

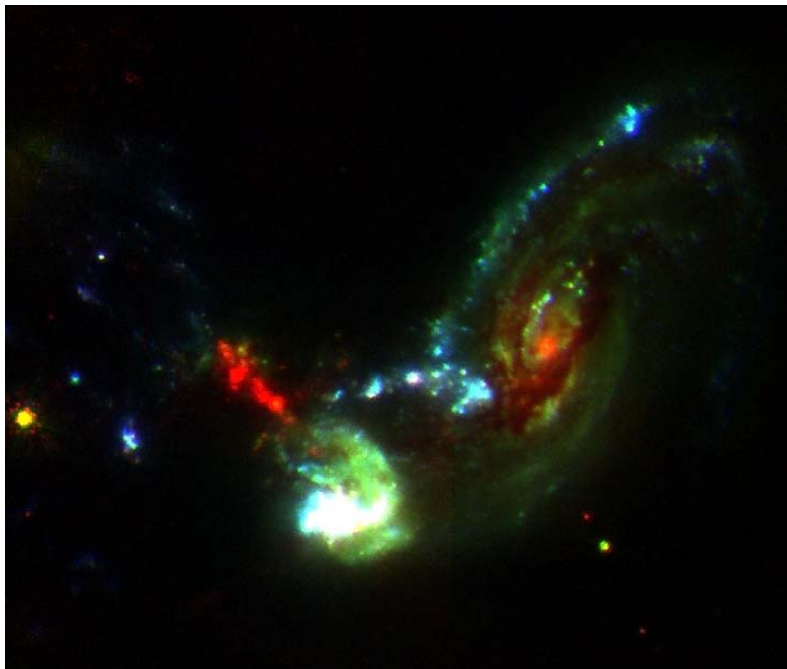


Figure 3. False-color RGB image of II Zw 096 made by combining the *HST* ACS SBC F140LP (blue), ACS F435W (green) and NICMOS F160W (red) data. North is up, East is to the left. The approximate size of this image is 40x30 arcsec, or 25x19 kpc. The source of nearly all the far-infrared emission is the Southernmost knot in the string of extremely red sources, left of center.

of both rapid stellar mass buildup and black hole growth in dusty galaxies. Spitzer has also given us our first look at the rest-frame mid-infrared spectral properties of samples of high-redshift ULIRGs and QSOs, strengthening the link between starbursts and AGN. GOALS is providing a multi-wavelength study of low-redshift LIRGs, in order to help us understand the processes that drive enhanced infrared emission in galaxies covering a much wider range in luminosity and merger state. The next generation of infrared space telescopes (Herschel, WISE, JWST, and the Japanese-led Space Infrared Telescope for Cosmology and Astrophysics - SPICA), together with ground-based sub-millimeter telescopes (ALMA, CCAT, LMT, etc.) will not only greatly expand our inventory of high-redshift LIRGs and ULIRGs, but also allow us to understand the physical conditions in these rapidly evolving galaxies at the earliest epochs.

Acknowledgments. We wish to thank the conference organizers for a stimulating meeting, and an exciting visit to Shanghai.

References

- Armus, L., et al. 2004, ApJS, 154, 178
- Armus, L., et al. 2006, ApJ, 640, 204
- Armus, L., et al. 2007, ApJ, 656, 148

- Armus, L., et al. 2009, PASP, submitted
Brandl, B.R. et al. 2006, ApJ, 653, 1129
Caputi, K.I., et al. 2007, ApJ, 660, 97
Charmandaris, V., Le Floch, E., & Mirabel, I.F. 2004, ApJ, 600, 15L
Daddi, E., et al. 2007, ApJ, 670, 173
Desai, V., et al. 2007, ApJ, 669, 810
Desai, V., et al. 2009, ApJ, submitted
Elbaz, D., & Cesarsky, C.J. 2003, Science, 300, 270
Evans, A.S., et al. 2008, ApJ, 675, 69L
Farrah, D., et al. 2007, ApJ, 667, 149
Farrah, D., et al. 2008, ApJ, 677, 957
Ferrarese, L. & Merritt, D. 2000, ApJ, 539, 9L
Gebhardt, K., et al. 2000, ApJ, 539, 13L
Genzel, R., et al. 1998, ApJ, 498, 579
Goldader, J.D., et al. 1997, AJ, 113, 1569
Goldader, J.D., et al. 2002, ApJ, 568, 651
Higdon, S.J.U., et al. 2006, ApJ, 648, 323
Heckman, T.M., Armus, L., & Miley 1990, ApJS, 74, 833
Heckman, T.M., Lehnert, M.D., Strickland, D.K., & Armus, L. 2000, ApJS, 129, 493
Hopkins, P.F., et al. 2007, ApJ, 659, 976
Howell, J.H., et al. 2009, ApJ, submitted
Houck, J.R., et al. 2004, ApJS, 154, 18
Houck, J.R., et al. 2005, ApJ, 622, 105L
Imanishi, M., et al. 2007, ApJS, 171, 721
Inami, H., et al. 2009, ApJ, submitted
Lo, K., Gao, Y., & Gruendl, R.A. 1997, ApJ, 475, 103L
Lutz, D., et al. 2008, ApJ, 684, 853L
Magnelli, B., et al. 2009, Astron. & Astrophys., in press.
Maggorian, J., et al. 1998, AJ, 115, 2285
Marshall, J.A., et al. 2007, ApJ, 670, 129
Menendez-Delemstre, K., et al. 2009, ApJ, in press
Meurer, G.R., Heckman, T.M., & Calzetti, D. 1999, ApJ, 521, 64
Papovich, C., et al. 2007, ApJ, 668, 45
Petric, A., et al. 2009, in preparation
Pope, A., et al. 2008, ApJ, 675, 1171
Rigby, J.R., et al. 2008, ApJ, 675, 262
Sajina, A., et al. 2007, ApJ, 664, 713
Sajina, A., et al. 2008, ApJ, 683, 659
Sanders, D.B., & Mirabel, I.F. 1996, ARA&A, 34, 749
Soifer, B.T., et al. 1984, ApJ, 283, 1L
Soifer, B.T., et al. 1986, ApJ, 303, 41L
Soltan, A. 1982, MNRAS, 200, 115
Spoon, H.W.W., et al. 2004, ApJS, 154, 184
Spoon, H.W.W., et al. 2006, ApJ, 638, 759
Spoon, H.W.W., et a. 2008, ApJ, 654, 49L
Spoon, H.W.W., et al. 2009, ApJ, 693, 1223
Sturm, E., et al. 2002, Astron. & Astrophys., 393, 821
Teplitz, H.I., et al. 2007, ApJ, 659, 941
Tran, Q.D., et al. 2001, ApJ, 552, 527
Valiante, E., et al. 2007, ApJ, 660, 1060
Walter, F., et al. 2009, Nature, 457, 699
Yan, L., et al. 2007, ApJ, 658, 778
Yu, Q., & Tremaine, S. 2002, MNRAS, 335, 965



Lee Armus



Lee Armus and Aaron Evans in the registration